Low-cost Condition Monitoring System for Smart Buildings and Industrial Applications

A. Toscani, N. Rocchi, D. Pinardi, M. Binelli, L. Saccenti, A. Farina, S. Pavoni and M. Vanali

***Abstract*—Condition Monitoring (CM) aims at damage identification through the measurement of various data collected from the systems under investigation (civil structures, mechanical parts, or industrial machineries) such as acceleration, temperature, displacement, and dynamic properties variation. Synchronization between the measured signals is mandatory for the processing of diagnostic metrics and modal analysis, which is why most of the monitoring systems today consist of a centralized acquisition unit to which analog transducers are connected. However, this solution entails a high cost of equipment and the use of long analog cables for each transducer. A full-digital network solution has been developed to solve these problems. The acquisition network is composed of Interface Boards for interfacing with the data storage system (e.g., a personal computer) and Acquisition Nodes integrating Micro Electro-Mechanical Systems (MEMS) digital triaxial accelerometers. The Interface Boards can be connected via Universal Serial Bus (USB) or Local Area Network (LAN), while the Acquisition Nodes are connected in daisy-chain via a digital bus implemented on an Unshielded Twisted Pair (UTP) cable. The proposed solution simplifies wiring, reduces system cost, and provides accurately synchronized signals. Experimental measurements on a truss model and a motor test bench for ball bearing failures diagnostic are presented, to demonstrate the effectiveness of the solution in civil and industrial applications, compared to a traditional analog laboratory-grade system.**

***Index Terms*—Bearing fault detection; Bridge monitoring; Building monitoring; Digital Network; Industrial Condition Monitoring; Low-cost sensors; MEMS accelerometers; Structural Health Monitoring.**

I. INTRODUCTION

In recent years, CM techniques [1], [2], [3] gained high importance in the field of maintenance of civil structures, industrial plants, and machines. The attention of the researchers is focused on the development of automatic damage detection algorithms capable of pointing out the presence of abnormal structural behavior, exploiting the information acquired by sensors placed on the monitored structures.

In the case of civil structures, a common approach consists in an operational modal analysis [4], [5] performed on the signals acquired by a distributed sensor network installed on the monitored structure, as in [6]. The purpose of this strategy is to detect the potential incoming damage through a variation in the dynamic properties of the system by relying on resonance frequencies or mode-shapes. In modal analysis techniques, the temporal alignment in the measured signals is mandatory [7], and therefore a direct analog link between the sensors and a centralized acquisition unit is a widely used solution. The use of long dedicated cables makes the wiring complex and massive, resulting in high installation and wiring costs, as mentioned in [8]–[11]. Other solutions based on Global Positioning System (GPS) are available but not suitable for networks installed inside road tunnels, mines, building interiors/foundations, wind turbines, and in all those places where GPS coverage is absent or not guaranteed, making the signal synchronization ineffective. Furthermore, it is not possible to achieve a "full wireless" operation inside interior spaces, due to the need for the power supply, which cannot be obtained using photovoltaic panels.

Moving to industrial production plants and machinery, CM is mainly focused on electric machines [12] and their components [13]. Among these, bearing faults are one of the most common [14], and may result in a reduction of performance and efficiency, overheating, and premature failure of the machinery. Bearing fault monitoring is traditionally based on routine inspections, due to the cost of the equipment and the need for sensors installed on the machinery. However, noninvasive fault diagnosis would be preferable, allowing for scheduled maintenance and minimized system downtime. By employing dedicated CM acquisition systems, fault conditions can be identified at incipient stage, thus preventing breakdowns [15]–[17]. Signal processing techniques must be capable of extracting the fault signatures, which usually have small amplitude, with respect to the background noise. For this purpose, the vibration signal is a well-known and proved effectiveness method [18]. Two of the most used metrics are the Root Mean Square (RMS) value of vibration velocity [19] and the Kurtosis [20].

Regarding the transducers, piezoelectric ones have been widely employed [21], thanks to their low self-noise [22], despite long analog cables are affected by signal degradation due to electromagnetic disturbances, often present in factories

This work was supported by ASK Industries S.p.A.

Funder: Project funded under the National Recovery and Resilience Plan (NRRP), Mission 4 Component 2 Investment 1.5 - Call for tender No. 3277 of 30/12/2021 of Italian Ministry of University and Research funded by the European Union - NextGenerationEU Award Number: Project code ECS_00000033, Concession Decree No. 1052 of 23/06/2022 adopted by the Italian Ministry of University and Research, CUP B33D21019790006, Ecosystem for Sustainable Transition of Emilia-Romagna (ECOSISTER).

(Corresponding author: A. Toscani).

A. Toscani, N. Rocchi, D. Pinardi, M. Binelli, L. Saccenti, A. Farina, S. Pavoni and M. Vanali are with the Department of Engineering and Architecture, University of Parma, Parma, 43124, Italy (e-mail: andrea.toscani@unipr.it; nicholas.rocchi@unipr.it; daniel.pinardi@unipr.it; marco.binelli@unipr.it; leonardo.saccenti@unipr.it; angelo.farina@unipr.it; stefano.pavoni@unipr.it; marcello.vanali@unipr.it).

and industrial plants [23]. Nowadays, instead, low-cost, digital MEMS transducers are often preferred [24]. They provide electromagnetic noise immunity, and their performance is constantly improving [25], [26].

In this paper, a novel idea is proposed to simplify the installation of a CM system, based on a local digital bus to collect data from several peripheral boards [27], ensuring the synchronism between all the signals. In addition, the design complexity and the cost of the proposed system are minimized with the use of digital MEMS accelerometers. Hence, neither Analog-to-Digital (A/D) converters nor programmable devices, e.g., microcontroller, Digital Signal Processor (DSP), or Field Programmable Gate Array (FPGA) are required. The complexity and the cost of the wiring are minimized too, since the communication takes place over a daisy-chain network implemented on UTP cables, thus avoiding bulky and expensive analog wiring between each transducer and the analog acquisition system. An extensive description of the proposed solution is presented in Section II. In Sections III and IV two experimental measurements and related results are described, while in Section V some use cases are presented. Eventually, conclusions are summarized in Section VI.

II. Acquisition System

The proposed CM system aims to overcome the previously mentioned issues by leveraging a distributed architecture. A block diagram of the proposed system is shown in Fig. 1. The acquisition system is composed by two main parts: an Interface Board (IB), shown in Fig. 2 (left), and a network of Acquisition Nodes (AN), shown in Fig. 2 (right), connected to the IB by means of the Automotive Audio Bus (A^2B) [28], [29]. The AN collect the sensor signals and send them to the IB. The AN are connected in daisy-chain [30] and each of them integrates a low-cost digital MEMS triaxial accelerometer. These two features reduce the complexity and the length of the cabling with respect to a traditional star topology. In addition, the wire is a single UTP, which can deliver both power supply and data, thus further reducing the cost.

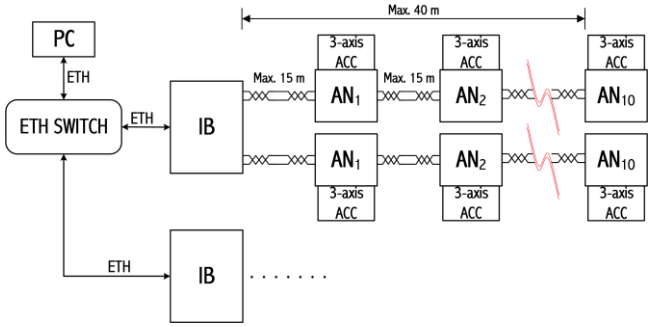

Fig. 1. Block diagram of the proposed CM system. Interface Boards (IB) are connected to a Personal Computer (PC) via ethernet cables, while Acquisition Nodes (AN) are connected over the A^2B bus.

The proposed CM system is highly modular and scalable, both in terms of number of sensors and dimensions. In fact, a single network can include up to 10 AN and a maximum number of signals equal to 32 at a sampling frequency (f_s) of 48 kHz [31]. As it can be seen in Fig. 1, the maximum distance between two adjacent AN is 15 m, while the total length of the network is 40 m, thus allowing to distribute the AN in wide areas, e.g., a building floor. Since the cable lengths may limit the field of application of the proposed CM system, the IB was developed to receive data from several A^2B networks (up to 4). In addition, many IBs can be connected through ethernet cables, thus exploiting, for example, an existing Local Area Network (LAN) infrastructure. Alternatively, the IB can transmit the data also via Universal Serial Bus (USB) for short distances.

Another fundamental benefit of the proposed architecture is the synchronization of the devices. In fact, the digital bus allows keeping synchronized all the AN of the network, with minimal latency and very low jitter levels [32]. Moreover, it is possible to temporally align the clock signals of the AN (with a resolution of about 20 ns) to compensate for the latency of the signal propagation through the nodes.

Fig. 2. Interface board (IB) of the proposed CM system (left). Acquisition node of the proposed CM system integrating a triaxial digital MEMS accelerometer (right).

III. Measurements On a Truss

A. Experimental Setup

A forced-response modal analysis was performed on a truss made of two H-beams of 4.2 m length and 13 aluminum rods. A front view of the structure model is shown in Fig. 3. One can note the transducer positions in correspondence of the numbered red markers.

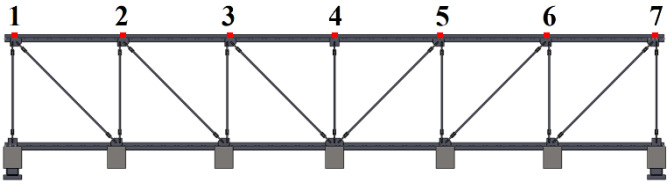

Fig. 3. Simplified model of the truss for forced-response modal analysis. Red dots represent the accelerometer positions.

The schematic of the experimental measurement is shown in Fig. 4. The response of the structure was recorded simultaneously with a standard analog system and with the proposed full-digital solution, both connected to a PC via USB. The system was excited along the vertical direction (Z axis) with a series of impulses provided to the structure with an impact hammer,

equipped with a load cell having a sensitivity of 0.99 pC/N, and connected to a charge amplifier. The output of the charge amplifier was split into two lines, one going to the analog system, and the other going to the analog input on the IB, thus allowing the same reference signal (load cell on impact hammer) to be recorded with both systems.

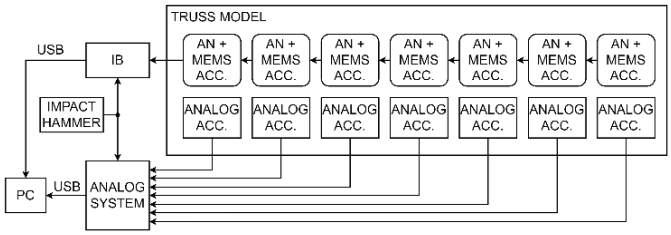

Fig. 4. Measurement schematic for the forced response analysis on a truss.

The analog system consisted of three acquisition boards and seven piezoelectric accelerometers, five of which were monoaxial and two triaxial, connected in a star topology. The digital system was made of one IB, operating at f_s = 48 kHz, and seven AN connected in daisy-chain. Each AN integrates a tri-axial MEMS accelerometer. Table I summarizes the main specifications of the employed transducers, where LSB means Least Significant Bit.

TABLE I
MAIN TRANSDUCERS SPECIFICATIONS

Accelerometer type	**Piezoelectric**	**MEMS**
Measurement Range Max	+/- 50 g peak	+/- 16 g peak
Maximum Output	+/- 5 V	+/- 8192 LSB
Noise PSD (100 Hz)	$3\ \mu g/\sqrt{Hz}$	$120\ \mu g/\sqrt{Hz}$
Noise (wide-band RMS)	0.1 mg	4 mg
Sensitivity	100 mV/g	500 LSB/g
Resolution	-	14 Bits

The piezoelectric and the MEMS accelerometers were positioned on the structure side-by-side. Each system recorded synchronously both the reference signal (load cell on impact hammer) and the accelerometer signals. Since the main interest was the information along the vertical axis, only the vertical direction (Z axis) of each triaxial accelerometer has been measured. Hence, a total number of eight signals was recorded by each system.

B. Experimental Results

In Fig. 5, the auto-spectrum of the load cell on the impact hammer is shown in the frequency range from 0 Hz to 1 kHz. The acceptable frequency range of the measurement is limited by a reduction of 20 dB in the impact hammer response, which corresponds to a reduction of an order of magnitude. Hence, the acceptable frequency range is comprised in the range 0 Hz – 650 Hz. Then, the Frequency Response Functions (FRF) between the impact hammer and the accelerometers were calculated for both measurements. In Fig. 6, the magnitude (above) and the phase (below) responses are shown for the accelerometer in the position two (see Fig. 3). It is possible to note an excellent similarity of the curves in the whole frequency range of interest.

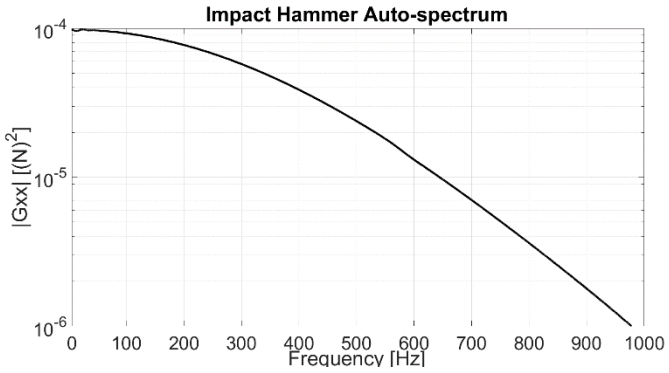

Fig. 5. Impact hammer load cell auto-spectrum.

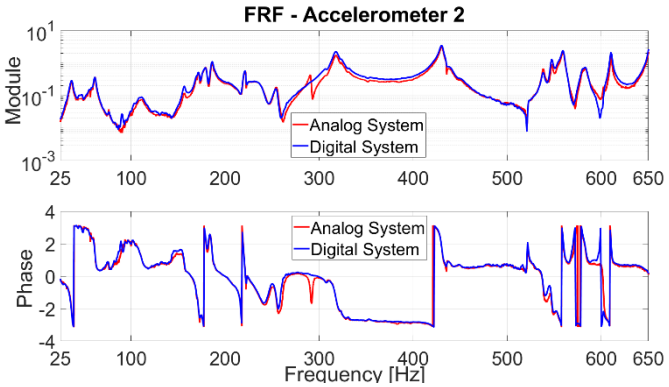

Fig. 6. FRF between impact hammer load cell and accelerometer n. 2, analog (red) and digital (blue) systems.

An experimental modal analysis was performed using a poly-reference least-squares complex frequency-domain method [33] and the stabilization diagram was calculated from the accelerometer FRF, for both analog and digital measurements. The aim of the analysis is the identification of the first two modes of the structure; hence, the frequency range was limited from 25 Hz to 70 Hz. In Fig. 7, the result is shown for the digital measurement. One can note that the two main modes are correctly identified.

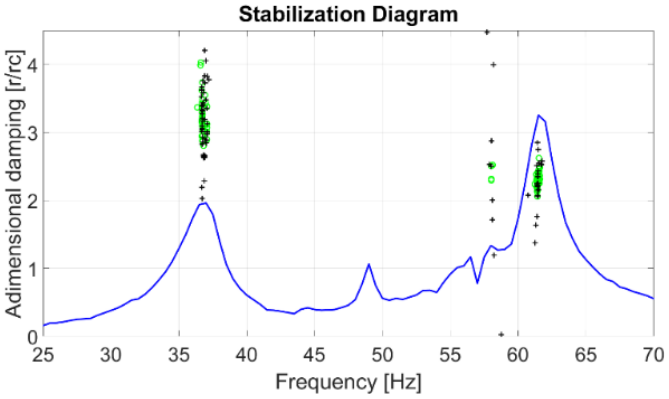

Fig. 7. Stabilization diagram for the digital measurement (green markers: stable poles; black markers: unstable poles).

Then, the structural model of the first two modes was calculated and it is shown in Fig. 8. One can note an excellent superimposition of the reconstructed curve (green) over the

experimental one (blue). Eventually, the first two modal frequencies were calculated on the analyzed accelerometer, for both analog and digital measurements. Results are summarized in Table II.

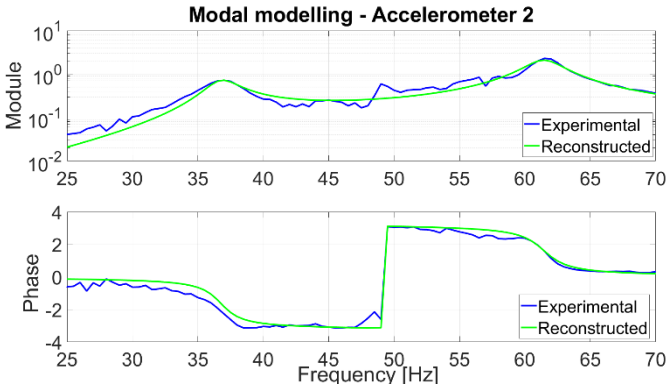

Fig. 8. Modal modelling on digital accelerometer n. 2.

TABLE II
FIRST TWO MODAL FREQUENCIES CALCULATED ON ACCELEROMETER N. 2 FOR ANALOG AND DIGITAL SYSTEMS

	First mode [Hz]	Second mode [Hz]
Analog System	36.7	61.6
Digital System	36.9	61.6

The mode shape is the most sensitive modal parameter to data synchronization since point movements and directions are strictly linked to phase in measurements. Therefore, mode shapes of the data obtained from both acquisition systems have been processed and compared through the Modal Assurance Criterion (MAC). MAC index can be interpreted as the normalized correlation coefficient between two vectors, and it allows detecting the similarity between two modes [34]. The MAC values are comprised between zero (no correlation) and one (perfect correlation). In Fig. 9, the MAC values show a perfect match between the first and second mode shapes detected by the two acquisition strategies.

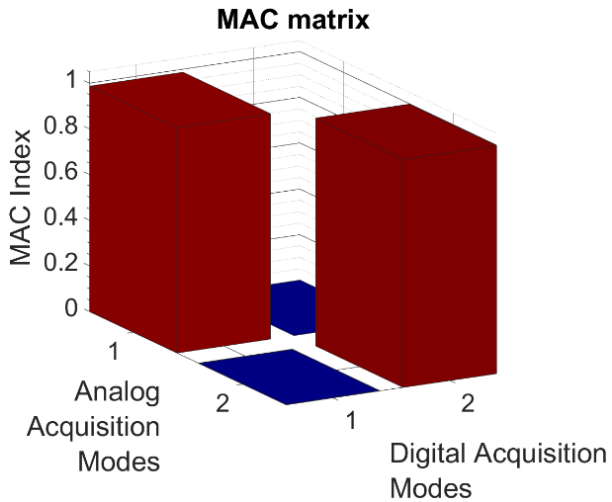

Fig. 9. MAC matrix between mode shapes processed from analog and digital acquisition systems.

IV. MEASUREMENTS ON A MOTOR TEST BENCH

A. Experimental Setup

The effectiveness of the proposed data acquisition system in an industrial application is provided through a bearing fault diagnosis using vibration signals. Radial bearings (Fig. 10) are widely used in every rotating machinery: they consist of two concentric rings with inner and outer races machined on them, separated by spherical or cylindrical rolling elements.

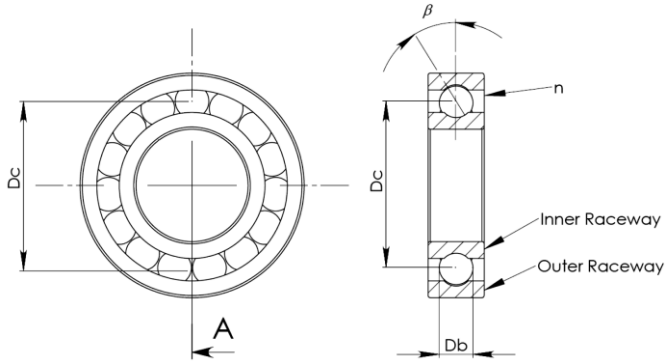

Fig. 10. Ball bearing structure, highlighting the characteristic dimensions.

Faults localized on different components of the bearing are responsible for different characteristic vibration components, that can be considered as fault signatures. These characteristic bearing fault frequencies depend on the geometry and the relative speed between the outer and the inner rings. The following equations are obtained by considering the outer ring fixed to the frame, so that the characteristic mechanical vibration frequencies can be calculated from the bearing's physical dimensions (Fig. 10):

$$F_{outer} = \frac{n}{2} F_r \cdot \left(1 - \frac{D_b \cos\beta}{D_c}\right) \quad (1)$$

$$F_{inner} = \frac{n}{2} F_r \cdot \left(1 + \frac{D_b \cos\beta}{D_c}\right) \quad (2)$$

$$F_{ball} = \frac{D_c}{D_b} F_r \cdot \left[1 - \left(\frac{D_b \cos\beta}{D_c}\right)^2\right] \quad (3)$$

where n is the number of rolling elements (i.e., spheres in the following), D_b is the rolling element diameter, D_c is the pitch diameter, β is the ball contact angle, which is 0 in absence of axial forces, and F_r is the rotation frequency of the machine.

The experimental measurements for bearing fault diagnosis using vibration signals were carried out on a motor test bench constituted of a welded steel rigid frame that houses a 6-poles induction machine (Fig. 11), directly connected to the three-phase main grid (400 V, 50 Hz). Table III summarizes the relevant nameplate data of the motor. The measurements were performed with the proposed digital data acquisition system and with an analog system. The digital system was constituted by an IB and four AN connected in daisy-chain topology, each of them embedding a triaxial MEMS accelerometer. Two triaxial and two monoaxial piezoelectric accelerometers were connected to the analog system in a star topology, as shown in the schematic of Fig. 12. The accelerometers were positioned as follows: one on

the motor test bench (Fig. 11, marker A), one directly on the motor (Fig. 11, marker B), one on the floor next to the motor test bench (Fig. 11, marker C), and one on the floor of an adjacent laboratory, at 10 m distance (position D not visible in Fig. 11). See Table I (Section III) for transducer specifications.

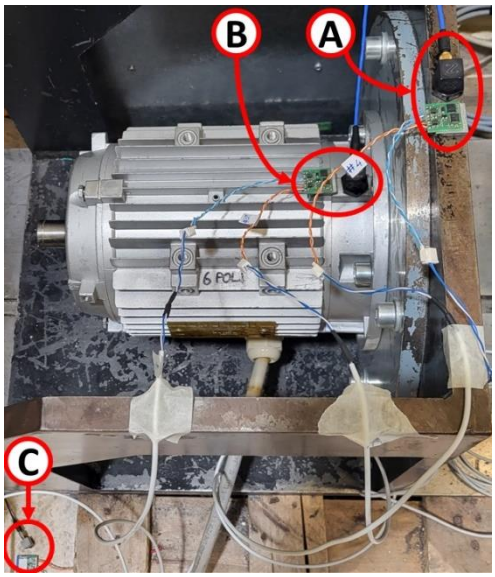

Fig. 11. Measurement schematic for the bearing fault diagnosis.

TABLE III
NAMEPLATE DATA OF THE MOTOR

Specification	Value
Nominal power	1100 W
Nominal current	2.8 A
Nominal frequency (*f*)	50 Hz
Number of poles	6
Nominal torque	11.5 Nm

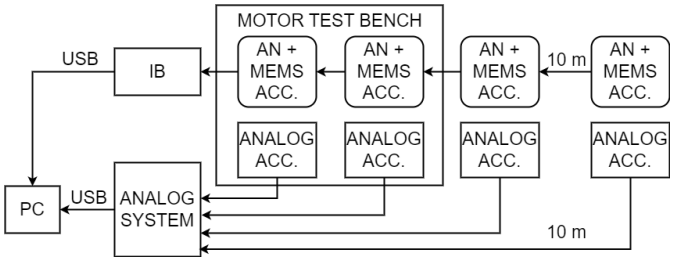

Fig. 12. Measurement schematic for the bearing fault diagnosis.

Different rolling bearing fault scenarios were employed to experimentally assess the performance of the proposed vibration monitoring system. At first, a reference measurement was taken on a bearing without any defects (brand new). Then, the drive end bearing was replaced with two artificially damaged samples:

- Single defect on the outer race. The defect was created by chemical etching of the bearing outer raceway. This type of fault reproduces a localized fault with only a characteristic signature at F_{outer}.
- Brinelling fault. The defect was created by applying a concentrated mechanical overload of 40 kN to the bearing. This type of fault involves all the three major components of the bearing, and it reproduces a more realistic scenario, characterized by the simultaneous presence of multiple characteristic vibration components at F_{outer}, F_{inner} and F_{ball}.

Table IV reports the specifications of the bearing used in the experiments and Table V summarizes the corresponding signature frequencies when the machine is operated with no load, at a speed of 998 Revolutions per Minute (RPM), that is F_r = *16.63 Hz*, and assuming $\beta = 0$. The operating speed was measured with a Compact A2103/LSR laser tachometer.

TABLE IV
SPECIFICATIONS OF THE EMPLOYED BALL BEARINGS

Specification	Value
Outer diameter	52 mm
Inner diameter	25 mm
Number of spheres *n*	9
Pitch diameter D_c	39.04 mm
Sphere diameter D_b	7.94 mm

TABLE V
EXPECTED FAULT FREQUENCIES OF THE EMPLOYED BALL BEARINGS

Specification	Value [Hz]
F_{outer}	59.6
F_{inner}	90.1
F_{ball}	78.4

B. Experimental Results

Each measurement consisted of a 60 s recording, performed at the same time with both digital and analog systems. The Power Spectral Density (PSD) was calculated for both the piezoelectric and the MEMS transducers, with a Hann window of 10 s and an overlap of 75%. Only the vertical axis (orthogonal to the rotation axis) was considered, being the direction of maximum excitation due to the bearing defects.

At first, the healthy bearing was analyzed (Fig. 13). The supply frequency component *f = 50 Hz* can be seen only on the piezoelectric transducer, as it is captured by the analog stage. Instead, the supply frequency 2nd harmonic *2f = 100 Hz* is present in the PSD of both transducers. The vibration frequency at twice the electrical line frequency is inherent for all alternating current electrical machinery vibration spectra and it is the result of a machine structure's excitation under the action of variable electromagnetic forces. The 3rd harmonic of the supply frequency *3f = 150 Hz* is again visible only on the piezoelectric transducer. Another two peaks are observed, corresponding to the mechanical speed of the motor, f_r and $2f_r$, as the result of a slight mechanical imbalance. From the comparison of the spectra, it is also possible to note that the noise floor of the MEMS transducer is one order of magnitude higher than the piezoelectric one, as it was expected from the specifications of the transducers (see Table I). Despite this, both types of transducers allowed correctly identifying the main information of the bearing under investigation.

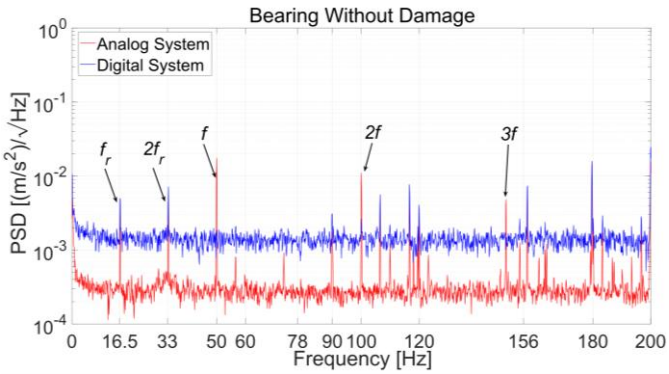

Fig. 13. PSD of the piezoelectric and MEMS accelerometers for a brand-new bearing.

Then, the PSD were calculated also for the damaged bearings. Fig. 14 shows the result for the single defect on the outer race of the bearing. The previously observed peaks are still present. In addition, the peaks at F_{outer}, $2F_{outer}$, and $3F_{outer}$ are clearly visible for both measurement systems.

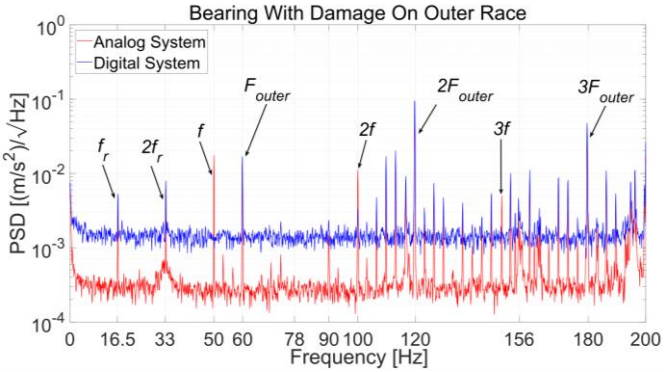

Fig. 14. PSD of the Piezo and MEMS accelerometers for a bearing with outer race damage.

Eventually, Fig. 15 shows the result for the brinelling damage, which causes several fault characteristic frequencies to appear at the same time, as described by (1), (2), and (3). As a notable difference in comparison to the previous single defect case, the spectra now exhibit a peak at F_{ball} and F_{inner} frequencies, and on the 2nd harmonics at $2F_{ball}$ and $2F_{inner}$.

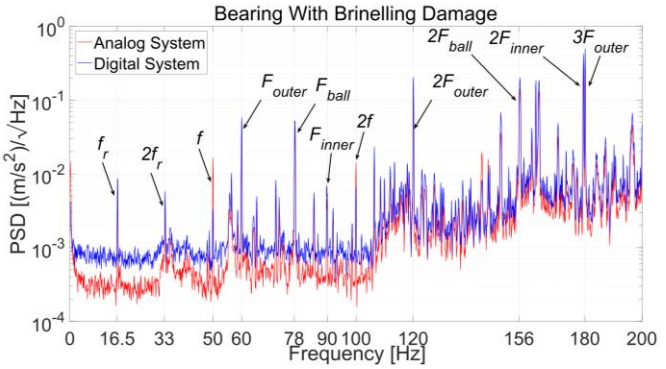

Fig. 15. PSD of the piezoelectric and MEMS accelerometers for a bearing with brinelling damage.

The synchronism of the measurement systems was evaluated with the cross-spectra G_{xy} and the coherence γ between the accelerometers on the motor (Fig. 11, marker B) and those positioned on the floor, next to the motor test bench (Fig. 11, marker C) and in the adjacent laboratory (marker D, not visible in Fig. 11). The vertical direction was considered, that is the Z axis. Results are shown in Fig. 16 and Fig. 17, for the Analog System (AS) and the Digital System (DS), in the case of the bearing with damage on the outer race. One can note an almost unitary coherence at F_{outer} (59.6 Hz) and $2F_{outer}$ (119.2 Hz). In correspondence of these frequencies, the cross-spectra exhibit the same phase.

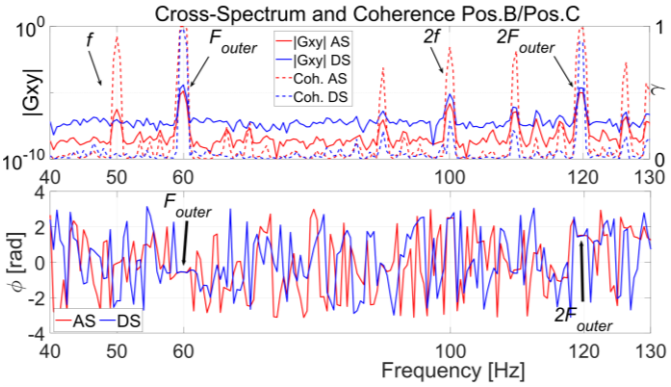

Fig. 16. Cross-spectra between accelerometers on the motor (pos. B) and on the floor next to the motor test bench (pos. C).

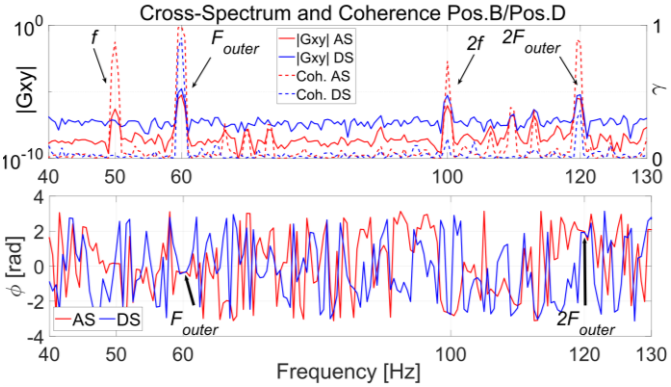

Fig. 17. Cross-spectra between accelerometers on the motor (pos. B) and on the floor in an adjacent laboratory (pos. D).

V. Possible Applications

The proposed system can be employed for performing a vibration-based CM of civil buildings, with great benefits for high-rise structures monitoring, as suggested in Fig. 18. In case of multiple floors, it is possible to use the ethernet LAN infrastructure to include additional IB and AN, thus extending the system capabilities. If the maximum distance between two IBs or between the IB and a PC is longer than 100 m (which is the limit of the ethernet over copper cables), there are two possible solutions: an ethernet switch to regenerate the signal every 100 m or an ethernet-to-fiber converter to transmit data over an optical fiber link.

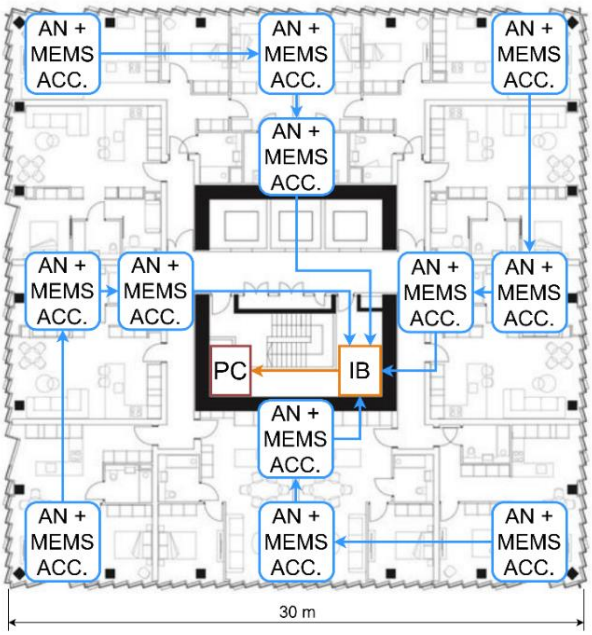

Fig. 18. Schematic of the proposed solution for a civil building (orange wire: LAN connection, blue wire: digital A^2B subnet over UTP).

The presented solution is also suitable for monitoring infrastructures like long bridges (Fig. 19). Most of the monitoring systems for this type of structure rely on two main strategies. The first one makes use of a single data acquisition node surrounded by a transducers network: the drawbacks are long and expensive cabling and extremely complex cable management. The second one includes multiple acquisition nodes distributed along the structure: in this case the drawbacks are the data synchronization between different acquisition nodes and a relevant increase in the equipment cost due to the high cost of each acquisition node. The proposed system provides an important step in the designing of monitoring systems for such structures since these issues are avoided. Moreover, the monitoring system upgrade with new transducers becomes significantly easier since the addition of further IB and/or AN does not require directly connecting the transducers to the data acquisition system with very long and expensive analog cables.

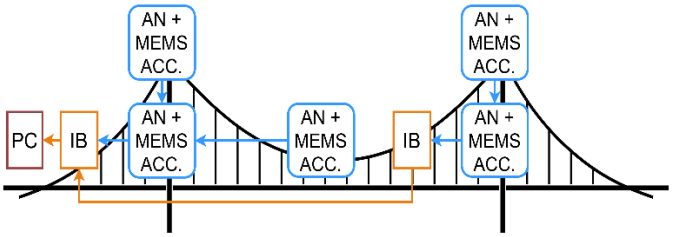

Fig. 19. Schematic of the proposed solution for a bridge (orange wire: LAN connection over fiber, blue wire: digital A^2B subnet over UTP).

A suitable employment for the proposed solution is related to industrial plants (Fig. 20). The main advancement, with respect to traditional solutions, consists in the possibility of sensing and monitoring several machineries or production line stations using multiple node networks. The usage of multiple IB allows for creating sensor subnetworks conveniently located next to the machineries to be monitored. If required, the monitoring system can be easily extended to other machinery, by adding additional AN and/or IBs. In addition, the usage of a digital bus makes the solution particularly appealing for any industrial applications, thanks to the inherent electromagnetic disturbance immunity.

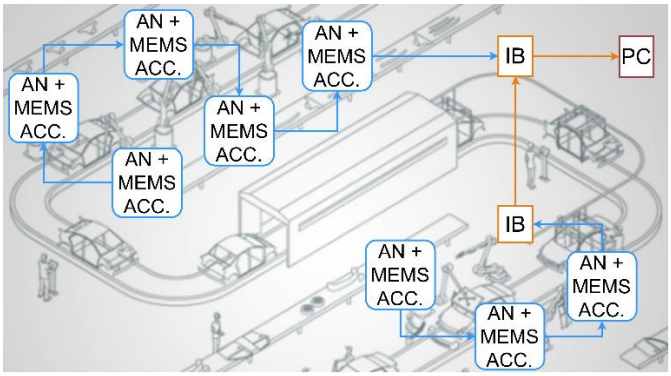

Fig. 20. Schematic of the proposed solution for an industrial power plant (orange wire: LAN connection over fiber, blue wire: digital A^2B subnet over UTP).

Eventually, the system can be employed for spot measurement in preliminary experimental tests, thanks to the easy and fast installation procedure. In [35], a flyover structure modal analysis has been performed by measuring accelerations on a bridge in the BreBeMi highway, a strategic infrastructure connecting the cities of Brescia, Bergamo, and Milano (Italy). The measurement system consisted of 30 accelerometers distributed among three spans with an overall length of 240 meters. In that case, the proposed system would have avoided the employment of several long and expensive cables, simplifying the installation and removal of the equipment.

VI. Conclusion

A full-digital, low-cost condition monitoring system for civil structures, infrastructures, and industrial applications was proposed. The described solution is based on an Interface Board and a series of Acquisition Nodes, connected to the Interface Board in daisy-chain topology through a digital bus. Each acquisition node integrates a digital MEMS triaxial accelerometer. The full-digital design, the adoption of MEMS transducers, and the cabling optimization allowed for minimizing the complexity, cost, and installation effort of the system.

A forced modal analysis experiment was carried out on a truss, using a traditional analog system based on piezoelectric transducers connected in star topology, in parallel with the proposed digital solution. The Frequency Response Functions between the impact hammer load cell and the accelerometers were calculated and compared for the two systems, showing excellent agreement. Then, a modal analysis was performed, demonstrating that the presented system provides identical results to the traditional one, especially in the evaluation of the mode shapes, which are the most sensitive modal parameters to the data synchronization.

A motor test bench was measured with three different ball bearings: a healthy one and two artificially damaged ones. Also in this case, the proposed digital solution featuring four AN and as many MEMS triaxial accelerometers was compared with a traditional analog system, featuring four piezoelectric accelerometers, two triaxial and two monoaxial. PSD for each case were calculated and compared in the frequency range 0 Hz – 200 Hz, showing an excellent agreement between the two solutions, despite a significant difference in the cost and quality of the sensors. It was possible to identify both artificial defects, as well as the healthy bearing, and the mechanical characteristic of the measurement system, such as the angular frequency.

Eventually, several application examples were provided, such as condition monitoring of long bridges, high-rise structures or large buildings, industrial machineries and plants, and preliminary measurement campaigns with temporary systems. In these cases, the solution presented in this paper would provide a series of advantages with respect to traditional systems. Among these, ensuring data synchronization, which is mandatory for modal analysis, fast and easy installation, highly demanded for temporary measurements, as well as possibility to easily upgrade the sensor network, together with a considerable reduction of cabling length, cost, and complexity, which make the system optimal for industrial applications.

REFERENCES

[1] C. R. Farrar and K. Worden, "An Introduction to Structural Health Monitoring," in *New Trends Vib Based Struct Health Monit*, K. Deraemaeker Arnaud and Worden, Ed. Vienna: Springer Vienna, 2010, pp. 1–17. doi: 10.1007/978-3-7091-0399-9_1.

[2] C. R. Farrar and K. Worden, *Structural Health Monitoring*. Wiley, 2012. doi: 10.1002/9781118443118.

[3] R. Hou and Y. Xia, "Review on the new development of vibration-based damage identification for civil engineering structures: 2010–2019," *J Sound Vib*, vol. 491, p. 115741, Jan. 2021, doi: 10.1016/j.jsv.2020.115741.

[4] C. Rainieri and G. Fabbrocino, *Operational Modal Analysis of Civil Engineering Structures*. New York, NY: Springer New York, 2014. doi: 10.1007/978-1-4939-0767-0.

[5] R. Brincker, L. Zhang, and P. Andersen, "Modal identification of output-only systems using frequency domain decomposition," *Smart Mater Struct*, vol. 10, no. 3, pp. 441–445, Jun. 2001, doi: 10.1088/0964-1726/10/3/303.

[6] M. Berardengo, F. Lucà, S. Manzoni, M. Vanali, and D. Acerbis, "Empirical Models for the Health Monitoring of High-Rise Buildings: The Case of Palazzo Lombardia," in *Topics in Modal Anal & Testing*, vol. 8, B. Dilworth and M. Mains, Eds. Cham: Springer International Publishing, 2021, pp. 169–175. doi: 10.1007/978-3-030-47717-2_16.

[7] S. Choi, B. Akin, M. M. Rahimian, and H. A. Toliyat, "Performance-Oriented Electric Motors Diagnostics in Modern Energy Conversion Systems," *IEEE Trans Ind Electron*, vol. 59, no. 2, pp. 1266–1277, Feb. 2012, doi: 10.1109/TIE.2011.2158037.

[8] A. Cigada, G. Moschioni, M. Vanali, and A. Caprioli, "The Measurement Network of the San Siro Meazza Stadium in Milan: Origin and Implementation of a New Data Acquisition Strategy for Structural Health Monitoring," *Exp Tech*, vol. 34, no. 1, pp. 70–81, Jan. 2010, doi: 10.1111/j.1747-1567.2009.00536.x.

[9] M. Berardengo, G. Busca, S. Grossi, S. Manzoni, and M. Vanali, "The Monitoring of Palazzo Lombardia in Milan," *Shock Vib*, vol. 2017, pp. 1–13, 2017, doi: 10.1155/2017/8932149.

[10] A. Cabboi, C. Gentile, M. Guidobaldi, and A. Saisi, "Continuous dynamic monitoring of historic masonry towers using few accelerometers: methodological aspects and typical results," in *7th Int Conf Struct Health Monit Intell Infrastructures*, Jul. 2015. [Online]. Available: https://www.researchgate.net/publication/315070472_Continuous_dynamic_monitoring_of_historic_masonry_towers_using_few_accelerometers_methodological_aspects_and_typical_results

[11] X. Y. Li, Y. H. Guan, S. S. Law, and W. Zhao, "Monitoring abnormal vibration and structural health conditions of an in-service structure from its SHM data," *J Sound Vib*, vol. 537, p. 117185, Oct. 2022, doi: 10.1016/j.jsv.2022.117185.

[12] A. Garcia-Perez, R. de J. Romero-Troncoso, E. Cabal-Yepez, and R. A. Osornio-Rios, "The Application of High-Resolution Spectral Analysis for Identifying Multiple Combined Faults in Induction Motors," *IEEE Trans Ind Electron*, vol. 58, no. 5, pp. 2002–2010, May 2011, doi: 10.1109/TIE.2010.2051398.

[13] A. H. Bonnett, "Root cause AC motor failure analysis with a focus on shaft failures," *IEEE Trans Ind Appl*, vol. 36, no. 5, pp. 1435–1448, 2000, doi: 10.1109/28.871294.

[14] ABB, "Motors don't just fail...do they? A guide to preventing failure.," 2015. https://new.abb.com/docs/librariesprovider53/about-downloads/motors_ebook.pdf

[15] J. R. Stack, T. G. Habetler, and R. G. Harley, "Fault signature modeling and detection of inner race bearing faults," in *IEEE Int Conf Elect Machines and Drives, 2005.*, 2005, pp. 271–277. doi: 10.1109/IEMDC.2005.195734.

[16] L. Frosini and E. Bassi, "Stator Current and Motor Efficiency as Indicators for Different Types of Bearing Faults in Induction Motors," *IEEE Trans Ind Electron*, vol. 57, no. 1, pp. 244–251, Jan. 2010, doi: 10.1109/TIE.2009.2026770.

[17] G. Curcurù, M. Cocconcelli, F. Immovilli, and R. Rubini, "On the detection of distributed roughness on ball bearings via stator current energy: experimental results," *Diagnostyka*, no. 3(51), pp. 17–21, 2009, [Online]. Available: https://bibliotekanauki.pl/articles/327844.pdf

[18] F. Lucà, S. Manzoni, A. Cigada, and L. Frate, "A vibration-based approach for health monitoring of tie-rods under uncertain environmental conditions," *Mech Syst Signal Process*, vol. 167, p. 108547, Mar. 2022, doi: 10.1016/j.ymssp.2021.108547.

[19] "ISO 20816-10:2016 Mechanical vibration — Measurement and evaluation of machine vibration." Interstate Council For Standardization, Metrology And Certification Std, 2016. [Online]. Available: https://www.iso.org/standard/63180.html

[20] R. B. Randall, *Vibration-based Condition Monitoring*. Wiley, 2011. doi: 10.1002/9780470977668.

[21] P. Jiao, K.-J. I. Egbe, Y. Xie, A. Matin Nazar, and A. H. Alavi, "Piezoelectric Sensing Techniques in Structural Health Monitoring: A State-of-the-Art Review," *Sensors*, vol. 20, no. 13, p. 3730, Jul. 2020, doi: 10.3390/s20133730.

[22] M. B. Moffett and J. M. Powers, "Noise in piezoelectric sensors," *J Acoust Soc Am*, vol. 88, no. S1, pp. S160–S160, Nov. 1990, doi: 10.1121/1.2028709.

[23] M. E. Haque, M. F. M. Zain, M. A. Hannan, M. Jamil, and M. H. Johari, "Transmission Loss Computed of Star Topology Sensor Network Base on DT, RED and SFQ Buffer Mechanism for Overseeing High Rise Building Structural Health," *Int J Biosci Biochem Bioinforma*, vol. 3, pp. 646–649, Jan. 2013, doi: 10.7763/IJBBB.2013.V3.294.

[24] M. Varanis, A. Silva, A. Mereles, and R. Pederiva, "MEMS accelerometers for mechanical vibrations analysis: a comprehensive review with applications," *J Braz Soc Mech Sci Eng*, vol. 40, no. 11, p. 527, Nov. 2018, doi: 10.1007/s40430-018-1445-5.

[25] S. Kavitha, R. Joseph Daniel, and K. Sumangala, "High performance MEMS accelerometers for concrete SHM applications and comparison with COTS accelerometers," *Mech Syst Signal Process*, vol. 66–67, pp. 410–424, Jan. 2016, doi: 10.1016/j.ymssp.2015.06.005.

[26] S. Thanagasundram and F. S. Schlindwein, "Comparison of integrated micro-electrical-mechanical system and piezoelectric accelerometers for machine condition monitoring," *Proc Inst Mech Eng, Part C: J Mech Eng Sci*, vol. 220, no. 8, pp. 1135–1146, Aug. 2006, doi: 10.1243/09544062C07405.

[27] A. Toscani *et al.*, "Low-cost Structural Health Monitoring System for Smart Buildings," in *2022 Second Int Conf Sustain Mobility Appl, Renewables Technol (SMART)*, Nov. 2022, pp. 1–7. doi: 10.1109/SMART55236.2022.9990379.

[28] Analog Devices, "A^2B Audio Bus: an Easier, Simpler Solution for Audio Design." https://www.analog.com/en/applications/technology/a2b-audio-bus.html

[29] M. Kessler, "Introducing the automotive audio bus (A^2B)," in *2017 AES Int Conf Automot Audio*, Aug. 2017, pp. 1–5. [Online]. Available: http://www.aes.org/e-lib/browse.cfm?elib=19187

[30] D. Pinardi *et al.*, "An Innovative Architecture of Full-Digital Microphone Arrays Over A^2B Network for Consumer Electronics," *IEEE Trans Consum Electron*, vol. 68, no. 3, pp. 200–208, Aug. 2022, doi: 10.1109/TCE.2022.3187453.

[31] N. Rocchi *et al.*, "A Modular, Low Latency, A^2B-based Architecture for Distributed Multichannel Full-Digital Audio Systems," in *2021 Immersive and 3D Audio: from Architecture to Automot (I3DA)*, Sep. 2021, pp. 1–8. doi: 10.1109/I3DA48870.2021.9610947.

[32] N. Rocchi, A. Toscani, G. Chiorboli, D. Pinardi, M. Binelli, and A. Farina, "Transducer Arrays over A^2B Networks in Industrial and Automotive Applications: Clock Propagation Measurements," *IEEE Access*, vol. 9, pp. 118232–118241, Aug. 2021, doi: 10.1109/ACCESS.2021.3106710.

[33] B. Peeters, H. van der Auweraer, P. Guillaume, and J. Leuridan, "The PolyMAX Frequency-Domain Method: A New Standard for Modal Parameter Estimation?," *Shock Vib*, vol. 11, no. 3–4, pp. 395–409, 2004, doi: 10.1155/2004/523692.

[34] A. Brandt, *Noise and Vibration Analysis*. Wiley, 2011. doi: 10.1002/9780470978160.

[35] G. Busca, A. Datteo, M. Paksoy, C. Pozzuoli, C. Segato, and M. Vanali, "Experimental vs Operational Modal Analysis: A Flyover Test Case," in *Dyn Civil Struct*, vol. 2, J. Caicedo and S. Pakzad, Eds. Cham: Springer International Publishing, 2015, pp. 365–377. doi: 10.1007/978-3-319-15248-6_39.

A. Toscani received the M.S. degree (cum laude) in electronic engineering and the Ph.D. degree in information technology from the University of Parma, Italy, in 2004 and 2008, respectively. His research activity is mainly focused on power electronics, high-performance electric drives, diagnostic techniques for industrial electric systems, and power converter for audio application. Since 2004, he has been working with the Department of Information Engineering (now, the Department of Engineering and Architecture), University of Parma, where he is currently a Research Fellow. Dr. Toscani is the author of two patents.

N. Rocchi received the B.S. and M.S. degrees (cum laude) in electronic engineering from the University of Parma, Italy, in 2017 and 2019, respectively. He is currently pursuing a Ph.D. degree in information technology at the University of Parma. His research interests include multichannel audio distribution, acquisition systems, and audio amplifiers.

D. Pinardi received the M.S. degree (cum laude) in mechanical engineering from the University of Parma, Italy, in July 2016, with a thesis on loudspeaker modeling, and the Ph.D. degree in industrial engineering from the University of Parma, in March 2020, with a thesis on the design of microphone, hydrophone, and camera arrays for spatial audio recording. He has been a Research Assistant of Prof. Angelo Farina at University of Parma since 2016, mainly specialized in spatial audio, design of transducer arrays, acoustics simulations and 3D auralization, applied to automotive field, and underwater acoustics.

M. Binelli received the B.S. and M.S. degrees in electronic engineering from the University of Parma, Italy, in 2003 and 2006, respectively, and the Ph.D. degree from the University of Parma, in 2010. His research interests include equalization, microphones and loudspeakers arrays, spatial audio psychoacoustics and active noise control. Since 2010, he has been working as a Research Fellow at the University of Parma.

L. Saccenti received the M.S. degree (cum laude) in electronic engineering from the University of Parma (Italy) in 2020 where he is currently pursuing the Ph.D. degree in Automotive for Intelligent Mobility. His research interests include acoustic simulation, 3D auralization, spatial audio and acoustical characterization of materials applied to automotive field.

A. Farina received the M.S. degree in civil engineering and the Ph.D. degree in technical physics from the University of Bologna, Italy, in 1982 and 1987, respectively. His research activity in applied acoustics includes noise and vibration, concert hall acoustics, simulation software, advanced measurement systems, microphone, and loudspeaker arrays. In May 2005, he became a Full Professor of environmental applied physics at the University of Parma. He is the author of more than 300 scientific papers. He was awarded by the Audio Engineering Society for his pioneering work on electroacoustic measurements with the exponential sine sweep.

S. Pavoni received the M.S. degree in mechanical engineering from the University of Parma, Italy, in March 2019, with a thesis on an automatic operational modal analysis (OMA) in presence of harmonic excitations. He is currently pursuing the Ph.D. degree in industrial engineering at the University of Parma. His research interests include Structural Health Monitoring (SHM), damage identification techniques and vibrations analysis.

M. Vanali received the M.S. degree in mechanical engineering and the Ph.D. degree in applied mechanics from Politecnico di Milano, Italy, in 1997 and 2003, respectively. Currently, he is an Associate Professor in mechanical measurements at the University of Parma. His research activity is mainly focused on SHM applications, sensors development, and vibration control/analysis.